Development of an Opposed Mass-Spring Type Bi-Stable Vibration Energy Harvesting System Using Stochastic Resonance

Linshi Guo[1], Wei Zhao[2], Nobuyuki Gomi[1], Jingchao Guan[1], Xilu Zhao[1, *]

[1]Department of Mechanical Engineering, Saitama Institute of Technology, Saitama, Japan

[2]Weichai Global Axis Technology Co., Ltd., Tokyo, Japan

Email address:

guolinshii@gmail.com (Linshi Guo), shunsuke0390@gmail.com (Wei Zhao), n_gomi@sit.ac.jp (Nobuyuki Gomi),
guanjingchao123@gmail.com (Jingchao Guan), zhaoxilu@sit.ac.jp (Xilu Zhao)

[*]Corresponding author

Abstract: Improving the efficiency of vibration power generation is an important research topic. Therefore, it is effective to develop a vibration power generation system using a bistable vibration model. The bistable vibration model considered in previous studies has the problem that the center of gravity is high and the vibration power generation efficiency is relatively low. In this study, we propose a horizontally opposed mass-spring type bi-stable vibration energy harvesting system that can be applied to low spaces. A bi-stable vibration system is built using horizontally opposed elastic springs and mass blocks. An elastic composite beam is constructed from an elastic bending plate and spring, and vibration power is generated using a piezoelectric element. An equation of motion is established accounting for the elastic composite beam, and a numerical analysis method based on the Runge-Kutta method is proposed. A formula for predicting the periodic excitation frequency at which stochastic resonance is most likely to occur is derived. A bi-stable vibration energy harvesting experimental device using a piezoelectric element is fabricated, and the proposed numerical analysis method and periodic excitation frequency prediction formula are validated. The amplitude increases and vibration power generation performance due to stochastic resonance are confirmed. In the verification experiment, it was confirmed that the vibration amplitude was expanded more than 7 times and the power generation amount increased by 21%.

Keywords: Ambient Energy, Bi-Stable Vibration System, Piezoelectric Element, Stochastic Resonance,
Vibration Energy Harvesting

1. Introduction

In a vibration energy harvesting system, increasing the vibration amplitude improves the power generation efficiency [1-5]. Therefore, it is advantageous to use a vibrating system with a natural frequency equal to the external excitation frequency, but this would be difficult under complex environmental vibrations [6-8].

To solve this problem, several linear vibration systems with different natural frequencies have been combined [9, 10], and a nonlinear vibration system that can be applied over a relatively wide frequency range has been proposed [11-13].

However, the vibrating device is complicated, and the obtained amplitude improvement is relatively small.

Therefore, stochastic resonance, which increases the amplitude of a vibration system in a random excitation environment, has attracted attention [14, 15]. In stochastic resonance, the vibration response is significantly amplified by applying a single-frequency vibration to a bi-stable vibration system in a random vibration environment [16-18]. To generate stochastic resonance in a mechanical system, three elements are required: a nonlinear bi-stable vibration system, random vibration, and periodic external force, the most important being the bi-stable vibration system [19, 20].
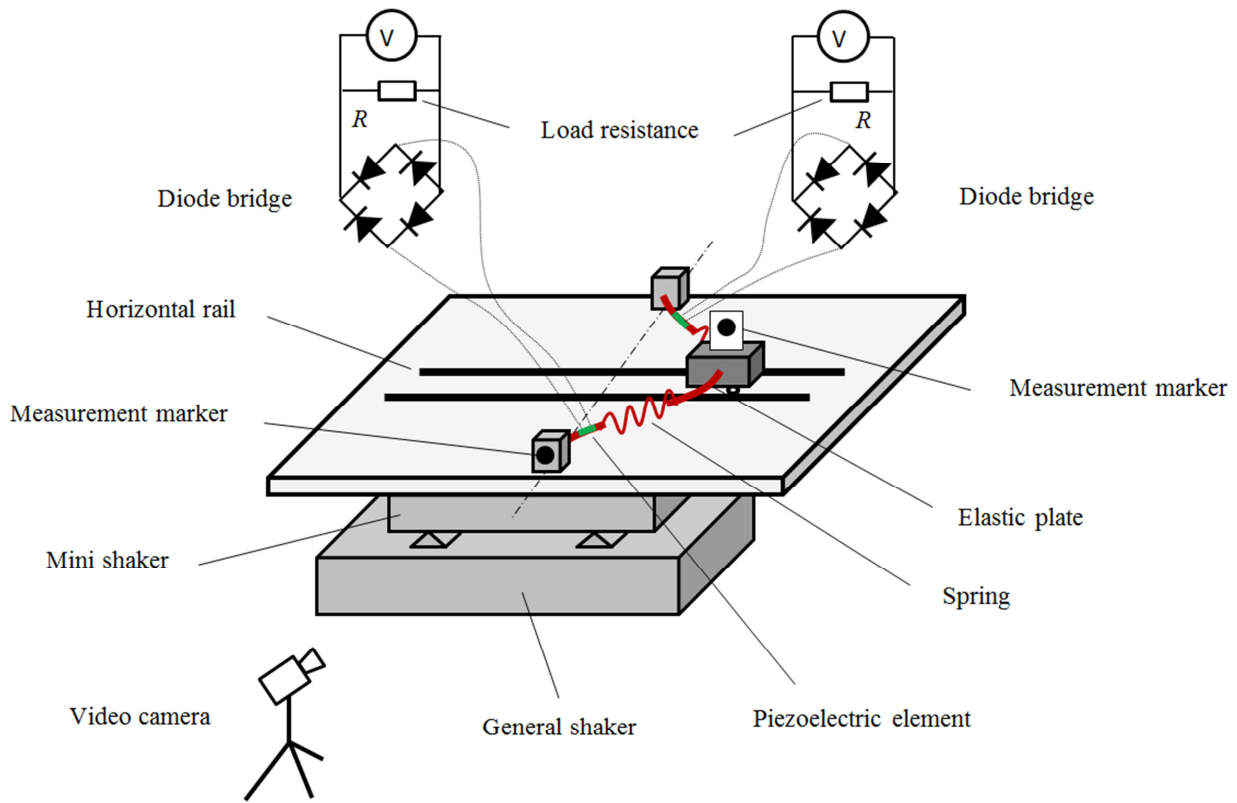
Figure 1. Diagram of the bi-stable vibration harvesting system.

In previous studies, the cantilever beam structure with a mass block at the tip was commonly used in a bistable vibration system [21]. To realize bi-stable vibration energy harvesting, a power generation device based on a bistable vibration system mounted on a low-speed vehicle tire has been developed [22].

However, in addition to a problem of durability of the bi-stable vibration system, the vibration range is small due to the elastic bending deformation of the cantilever beam [23].

A bistable vibration model composed of elastic springs and mass blocks has been proposed to study bi-stable vibration systems with larger amplitudes [24]. However, this model is difficult to apply to low spaces.

In this study, we propose a horizontally opposed bi-stable vibration energy harvesting system using piezoelectric elements. An elastic composite beam is assembled using an elastic bending plate and a spring, and is combined with a piezoelectric element to realize vibration power generation. An equation of motion for a system accounting for elastic composite beams is established, and a numerical analysis method using the Runge-Kutta method is proposed. An equation predicting the periodic excitation frequency at which stochastic resonance is most likely to occur is derived. We build a bi-stable vibration-energy-harvesting experimental device and perform measurements of the performance of stochastic resonance and vibration power generation. We validate the proposed numerical analysis method and the predicted excitation frequency that causes stochastic resonance, and evaluate the amplitude increase and vibration power

generation performance due to stochastic resonance.

2. Materials and Methods

2.1. Bi-Stable Vibration Energy Harvesting System

We propose a bistable vibration energy harvesting system, as shown in figure 1. A mass block moves along the horizontal rails. An elastic composite beam consisting of elastic springs and thin elastic bending plates is installed between the mass block and supports on both sides. Both ends of the composite elastic beam are fixed to the mass block and support base. A piezoelectric element is attached to the surface of the elastic bending plate. An alternating voltage is generated from the piezoelectric element that deforms with the elastic bending plate. A rectified voltage is produced using a diode bridge circuit. The electrical load resistance of the measuring circuit is 1.0 MΩ.

Figure 2 shows the analysis model extracted from the bi-stable vibration system. x_d is the distance from the central axis to the mass block. x_t is the distance from the central axis to the fixed base. x is the relative displacement of the mass block with respect to the fixed base. h is the vertical distance between the upper and lower fixing points of the elastic bending plate. F_s denotes the restoring force of the elastic spring. The elastic composite beam is assumed to be vertically symmetrical, and the horizontal deflection x_b of the elastic beam due to bending is assumed to be constant. The restoring force of the elastic spring lies approximately along the straight line connecting the upper and lower fixed points.
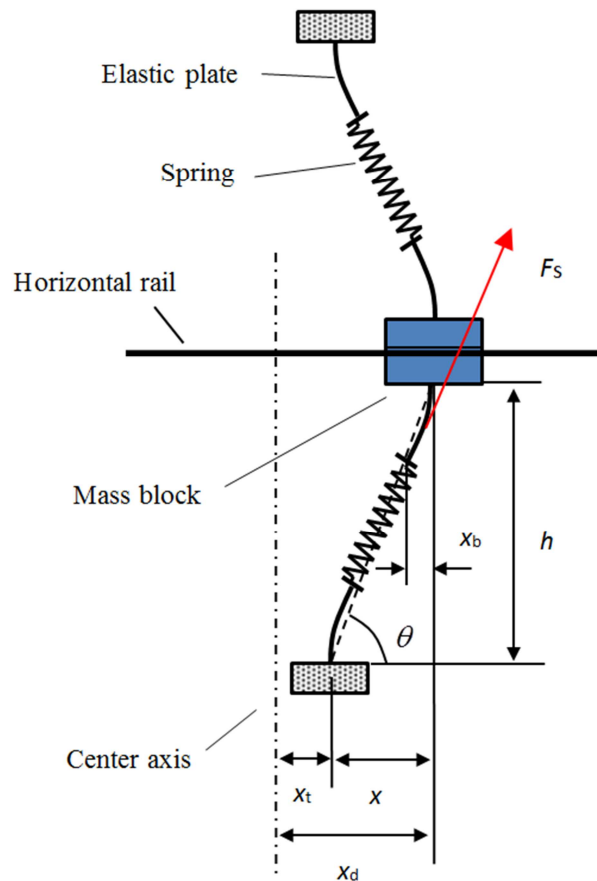
Figure 2. *Vibrating model of the bi-stable vibration harvesting system.*

Figure 3 shows the experimental bi-stable vibration energy harvesting device. A mini-shaker is attached under the vibration system, and a single-frequency external force is applied from the mini-shaker. An experimental device consisting of a vibration system and a mini shaker is fixed on the upper surface of the general shaker, which applies random vibration.
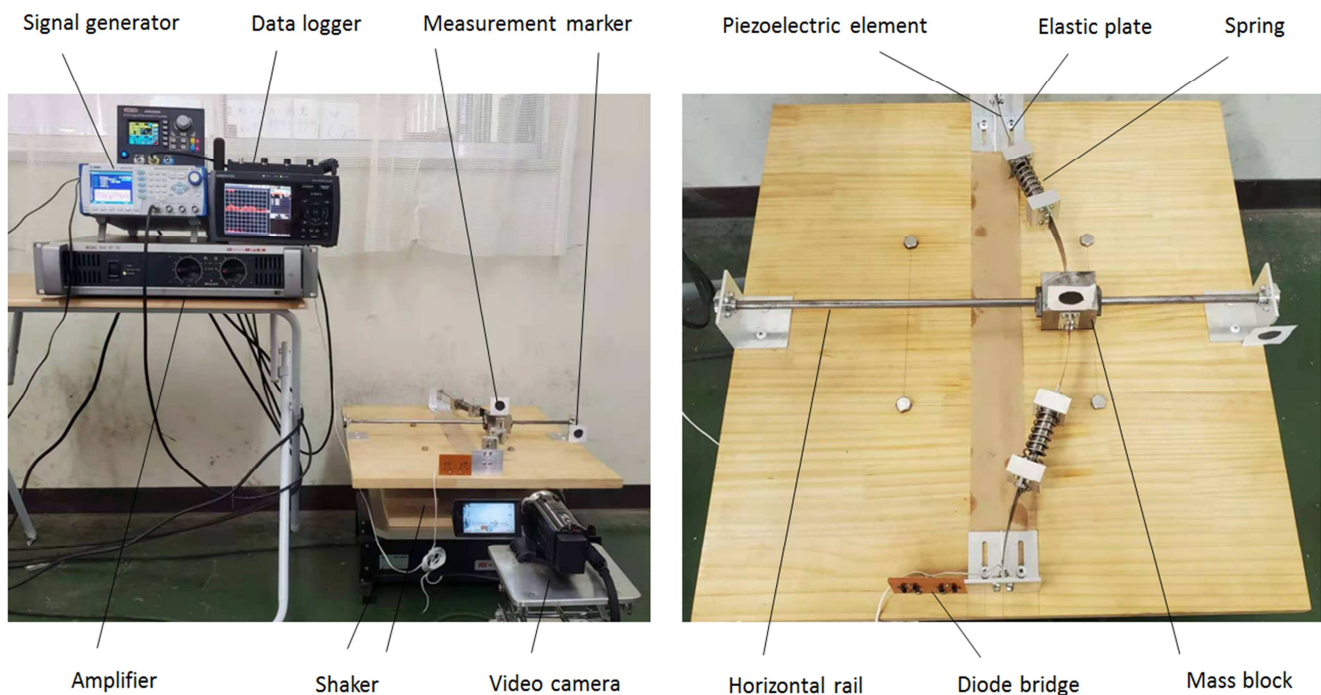

Figure 3. *Experimental setup and measurement system of the bi-stable vibration harvesting system.*
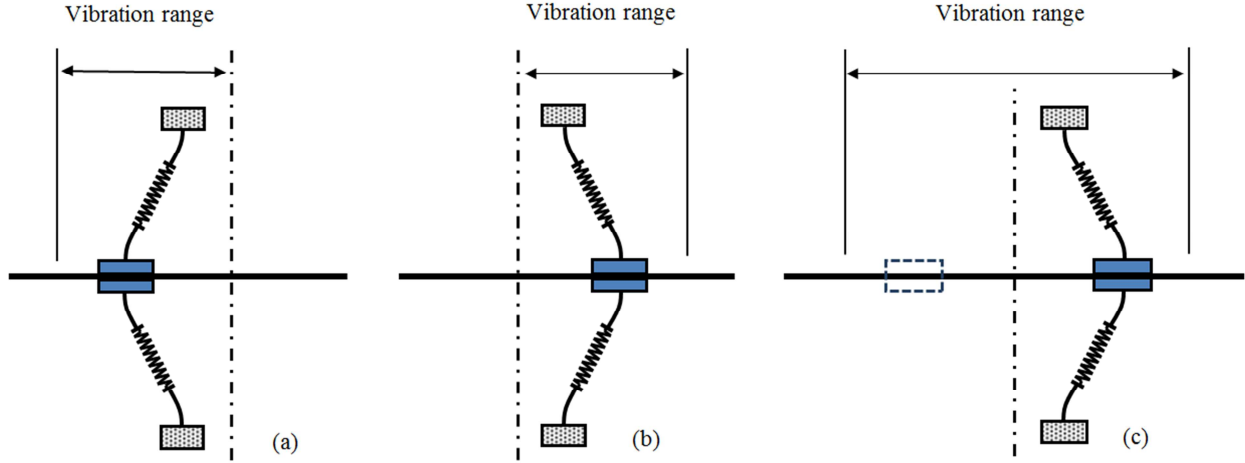
Figure 4. *Three stable vibration states: (a) left-side mono-stable vibration, (b) right-side mono-stable vibration, and (c) bi-stable vibration.*

To measure the vibration displacement, measurement markers are attached to the mass block and fixed base. A high-speed video camera is used to record the motion trajectory of the measurement marker, and tracking processing software is used to create time-series vibration displacement data. The lead wire of the piezoelectric element is connected to the data logger through the diode bridge circuit, and the voltage of the vibration power generation is recorded.

Table 1 shows the detailed parameters of the bistable vibration energy harvesting experimental device and measurement system used in this study.

Table 1. *Specifications of the experimental setup of the bi-stable vibration energy harvesting system.*

Items	Specifications
Mass block	Mass 605 g
Horizontal rail	Length 350 mm, Width 50 mm
Distance in the plane	From rail to support base 200 mm
Elastic spring	Spring constant 295 N/m, Initial length 90 mm
Elastic bending plate	Size 90×20×0.3 mm, Young's modulus 210 GPa
Piezoelectric element	K7520BS3 (Thrive Co., Ltd)
Diode	D1NS6-5060 (SHINDENGEN Co., Ltd)
Mini shaker	SSV-105 (SAN ESU Co., Ltd)
General shaker	SSV-125 (SAN ESU Co., Ltd)
Amplifier	SVA-ST-30 (SAN ESU Co., Ltd)
Function generator	NF-WF1973 (NF Corporation)
Video camera	GZ-E765 (JVC Co., Ltd)，FPS=300
Marker tracking system	MOVIS V3.0 (NAC Image Technology Inc.)

As shown in figure 2, the initial length of the elastic composite beam at rest is larger than h; therefore, there is one equilibrium position on each side of the mass block at rest.

As shown in figure 4, there are three vibration states for the mass block. Figure 4(a) shows the vibration state centered at the left-side equilibrium position. Figure 4(b) shows the vibration state centered at the right-side equilibrium position. Figure 4(c) shows the vibration state that passes through the central symmetry axis and straddles the left and right equilibrium positions. Vibrations around a single equilibrium position, as shown in figures 4(a) and (b), are called monostable oscillations. Oscillation between two equilibrium positions, as shown in figure 4(c), is called bi-stable oscillation.

2.2. Analysis Method

From figure 2, the horizontal motion equation of the mass block is expressed as.

$$m\ddot{x}_d + c\left(\dot{x}_d - \dot{x}_t\right) + 4K_b x_b + 2F_s \cos\theta = 0 \qquad (1)$$

where K_b denotes the stiffness coefficient of the thin elastic bending plate, and c is the damping coefficient. The relative displacement x of the mass block with respect to the fixed base is expressed as.

$$x = x_d - x_t \qquad (2)$$

Substituting equation (2) into equation (1), the equation of motion is as follows:

$$m\ddot{x} + c\dot{x} + 4K_b x_b + 2F_s \cos\theta = -m\ddot{x}_t \qquad (3)$$

From figure 2, the tilt angle is expressed as follows.

$$\cos\theta = \frac{x}{\sqrt{x^2 + h^2}} \qquad (4)$$

Ignoring the change in length of the elastically bent plate during the vibration process, the deflection of the elastically bent plate can be approximated with the following expression:

$$x_b = l_b \cos\theta \qquad (5)$$

The elastic force of the spring is given by

$$F_s = K_s \left(\sqrt{x^2 + h^2} - 2l_b - l_s\right) \qquad (6)$$

where K_s and l_s are the elastic modulus and free length of the spring, respectively. The elastic modulus of an elastically bent plate can be calculated using the following equation [25].

$$K_b = \frac{3EI}{l_b^3} \qquad (7)$$

where E is the Young's modulus of the material, and I denote the area moment of inertia. By substituting equations (4)–(7) into equation (3), the equation of motion can be expressed as follows:

$$m\ddot{x} + c\dot{x} + \left[1 - 2K_s \left(2l_b + l_s - \frac{6EI}{K_s l_b^2} \right) \frac{1}{\sqrt{x^2 + h^2}} \right] x = -m\ddot{x}_t \quad (8)$$

The equivalent length of the elastic composite beam is given by

$$l_e = 2l_b + l_s - \frac{6EI}{K_s l_b^2} \quad (9)$$

Therefore, the equation of motion (8) is expressed as follows.

$$m\ddot{x} + c\dot{x} + 2K_s \left(1 - \frac{l_e}{\sqrt{x^2 + h^2}} \right) x = -m\ddot{x}_t \quad (10)$$

The potential energy of the vibrating system is given by

$$U = K_s \left(x^2 - 2l_e \sqrt{x^2 + h^2} \right) \quad (11)$$

To investigate the distribution characteristics of the potential energy, we solve equation (12):

$$\frac{dU}{dX} = 2K_s \left(1 - \frac{l_e}{\sqrt{x^2 + h^2}} \right) x = 0 \quad (12)$$

Three solutions are obtained, as expressed in (13).

$$x_0 = 0 \quad x_1 = -\sqrt{l_e^2 - h^2} \quad x_2 = \sqrt{l_e^2 - h^2} \quad (13)$$

The potential energy distribution in equation (11) is represented in Figure 5. x_0, x_1, and x_2 in Equation (13) are the extrema of the potential energy, and correspond to the three equilibrium positions of the mass block. ΔU is the potential energy barrier of vibration of the mass block.

When the mass block vibrates, it oscillates in a single stable motion on the left or right side if the sum of the kinetic and potential energies does not exceed the barrier value. When the sum exceeds the barrier value, the mass block crosses the central axis, and bi-stable vibration occurs.
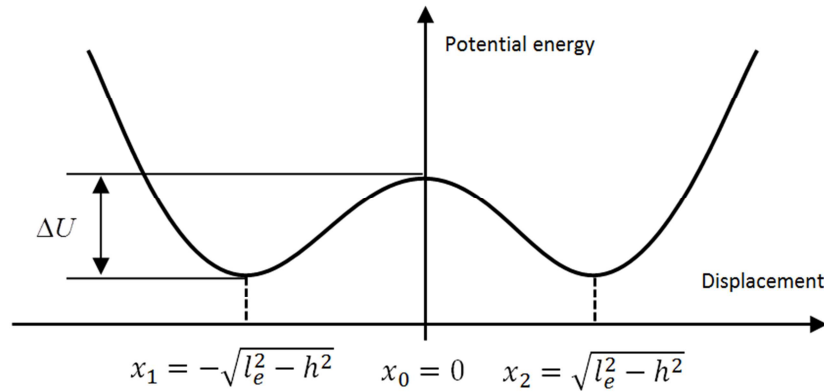

Figure 5. *Distribution characteristics of potential energy for the bi-stable vibration system.*

When random excitation is applied to a bistable vibration system, the mass block oscillates often mono-stably on the right or left sides of the central axis. When random and periodic external forces are applied simultaneously, the vibration of the mass block turns into bistable vibration, and resonance with a large amplitude occurs. This type of resonance is called stochastic resonance because the random vibration environment contains uncertain factors [16].

Applying the Runge-Kutta method to equation (10) yields the relative displacement x_i. By adding the excitation displacement x_{ti} of the support table to the relative displacement x_i, the absolute displacement x_{di} of the mass block can be calculated as follows:

$$x_{di} = x_i + x_{ti} \quad i = 1, 2, \cdots, n \quad (14)$$

Before performing the vibration analysis, it is necessary to determine the damping coefficient c of the vibration model; this is performed using the following procedure:

First, the vibration system is excited by a sinusoidal signal (1.8 Hz in this experiment), and the vibration displacement of the mass block is measured. Next, a provisional damping factor is set. Then, a vibration analysis is performed, and the analytical solution and measured value of the vibration displacement are compared.

If the error satisfies the convergence criterion (error in relative displacement is 0.01% or less), the damping coefficient is obtained, and the identification is terminated. If the error does not satisfy the convergence criterion, the damping coefficient is adjusted, and vibration and accuracy checks are performed again.

This analysis and checking process are repeated until the convergence criterion is met.

Figure 6 shows the results obtained by identifying the bistable vibration model used in this study. The analytical and measured response displacements agree. The corresponding damping coefficient is $c=1.92$ Ns/m. In addition, as a result of

identification using other sine waves with excitation frequencies between 1.0 Hz and 3.0 Hz, it is confirmed that the
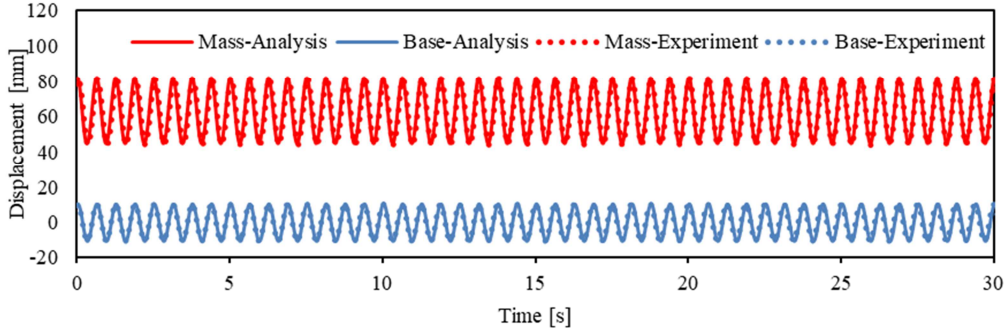
damping coefficient c is almost unchanged.

Figure 6. *Displacement results for the identification of the damping coefficient.*

2.3. Conditions for Stochastic Resonance

Stochastic resonance can be generated by exciting a bi-stable vibration model in a random excitation environment with a periodic excitation signal. The periodic excitation frequency at which the stochastic resonance is likely to occur can be predicted by the following equation [16]:

$$f_k = \frac{w_b w_0}{4\pi q} \exp\left(-\frac{\Delta \bar{U}}{D}\right) \quad (15)$$

where w_b and w_0 are the natural angular frequencies at the extreme points of the potential energy, respectively. By differentiating the potential energy equation (11) and using equation (13), w_b and w_0 can be calculated as follows:

$$w_b = \sqrt{\frac{\left|U''\left(\sqrt{l_e^2 - h^2}\right)\right|}{m}} = \sqrt{\frac{2K_s}{m}\left(1 - \frac{h^2}{l_e^2}\right)} \quad (16)$$

$$w_0 = \sqrt{\frac{|U''(0)|}{m}} = \sqrt{\frac{2K_s}{m}\left(\frac{l_e}{h} - 1\right)} \quad (17)$$

l_e is the equivalent length of an elastic composite beam and is calculated using equation (9). Q is the damping parameter, which is calculated using the following equation:

$$q = \frac{c}{m} \quad (18)$$

The potential energy barrier per unit mass is expressed as follows:

$$\Delta \bar{U} = \frac{K_s}{m}\left(\bar{l} - h\right)^2 \quad (19)$$

By substituting equations (16) – (19) into equation (15), the prediction equation for the periodic excitation frequency at which stochastic resonance is likely to occur is expressed as follows:

$$f_k = \frac{K_s\left(l_e - h\right)}{2\pi c l_e} \sqrt{\frac{l_e + h}{h}} \exp\left(-\frac{K_s\left(l_e - h\right)^2}{mD}\right) \quad (20)$$

Using the parameters of the bistable motion system shown in table 1 and equation (9), the equivalent length of the elastic composite beam is obtained using the following equation:

$$l_e = 2l_b + l_s - \frac{Eb_b h_b^3}{2K_s l_b^2} = 0.246\,m \quad (21)$$

The signal intensity D of the random excitation is obtained from the kinetic energy per unit mass. After measuring the vibration velocity while vibrating with only a random signal, the signal strength can be calculated using the following equation:

$$D = \frac{1}{2N}\sum_{i=1}^{N}\left(v_i - v_{aver}\right)^2 \quad (22)$$

where vi denotes the vibration velocity, vaver denotes the average vibration velocity, and N denotes the number of sample points in the measurement experiment. By substituting the actual measured values into equation (22), the signal strength of the random excitation (D=0.785 J/kg) is obtained.

From equation (20), the predicted value of the periodic excitation frequency at which stochastic resonance is likely to occur is given by:

$$f_k = 2.64\,Hz \quad (23)$$

3. Results and Discussion

Based on the predicted excitation frequency given by (23), the frequency of the periodic excitation signal used in the experiment was set from 2.0 Hz to 3.2 Hz with intervals of 0.3 Hz. The amplitude of the periodic excitation signal was set at 20 mm.

Figures 7–17 show the measurement results for each case. The black solid line indicates the vibration displacement of the mass block, the blue dotted line indicates the vibration displacement of the support base, and the red solid line

indicates the voltage of the vibration power generation. The voltage of the vibration power generation is positive because it is rectified by a diode bridge circuit.

3.1. Excitation by Random Signal

In the case of the random excitation shown in figure 7, the vibration response displacement of the mass block is relatively small, and the mass block vibrates mono-stably on the left side of the central axis. The voltage fluctuates randomly according to the change in the amplitude of the random vibration. The maximum voltage is 13.84 V, and the average is 2.73 V. There is no extremely large peak voltage value.
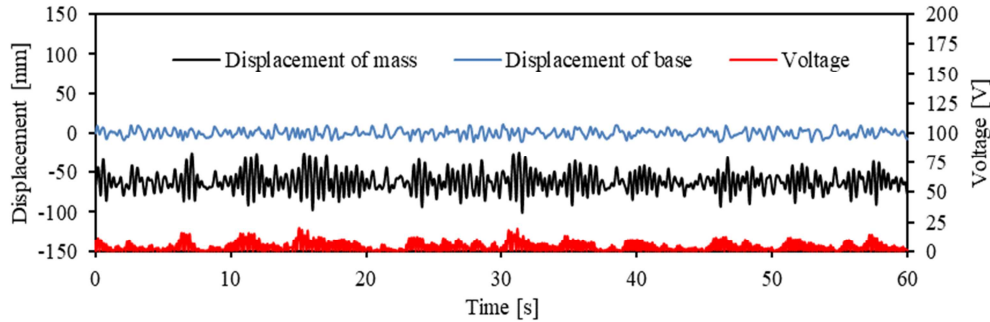

Figure 7. Experiment results of vibration displacements and voltage excited only with random force.

3.2. Excitation by Periodic Signal

As shown in figure 8, the vibration displacement of the mass block when it is excited at a low frequency of 2.0 Hz is slightly larger than that of the support. The voltage value associated with a change in vibration displacement is relatively small, with a maximum value of 4.74 V and an average value of 2.55 V.
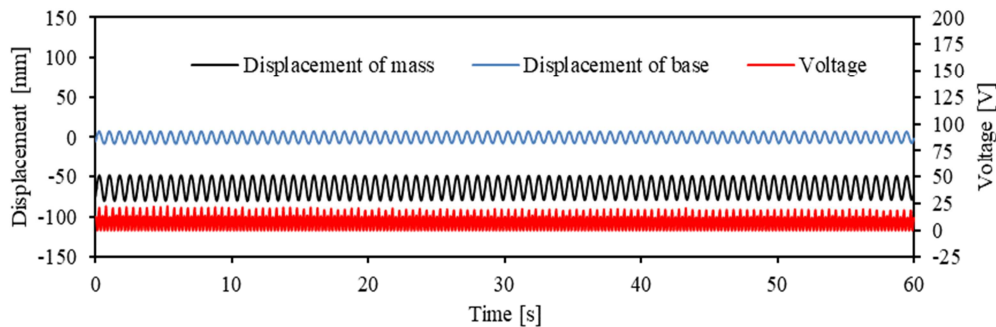

Figure 8. Experimental results of vibration displacements and voltage excited with 2.0 Hz periodic forces.

Figures 9–11 show the measurement results at frequencies of 2.3, 2.6, and 2.9 Hz. The maximum voltages are 7.92, 16.32 and 14.44 V, and the average values are 4.37, 9.43 and 8.50 V, respectively. There is an apparent natural vibration mode, and the mass block vibrates with an amplitude larger than that of the vibration displacement of the support.

Compared to the results of the low-frequency (2.0 Hz) excitation, the voltage increases with increasing amplitude.

When vibration is applied at a relatively high frequency (3.2 Hz), as shown in figure 12, the amplitude and motion velocity decrease again, and the voltage value also to decreases. The maximum voltage is 12.04 V, and the average is 7.29 V.
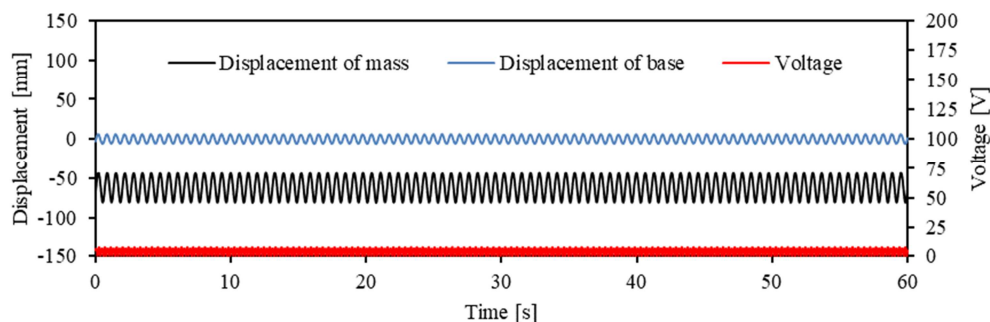

Figure 9. Experimental results of vibration displacements and voltage excited with 2.3 Hz periodic forces.
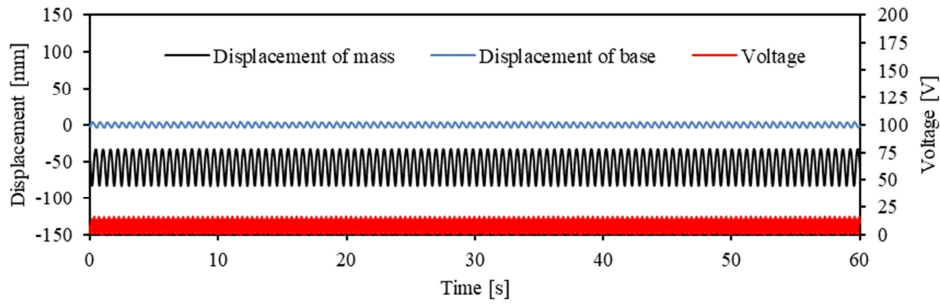
Figure 10. Experimental results of vibration displacements and voltage excited with 2.6 Hz periodic forces.
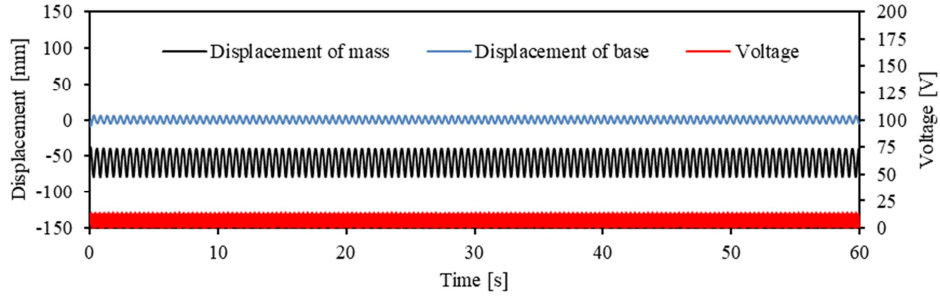

Figure 11. Experimental results of vibration displacements and voltage excited with 2.9 Hz periodic forces.
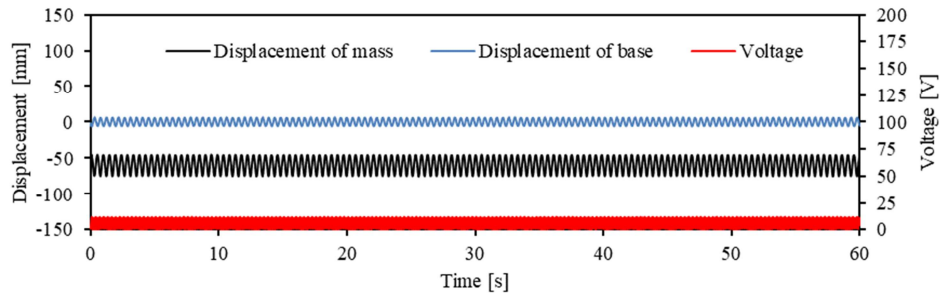

Figure 12. Experimental results of vibration displacements and voltage excited with 3.2 Hz periodic forces.

3.3. Joint Excitation of Random and Periodic Signals

Figure 13 shows the measurement results under simultaneous excitation by the random and periodic signals at a frequency of 2.0 Hz. The vibration displacement of the mass block is slightly larger than that of the support base, and the amplitude is a randomly fluctuating single-stable vibration. The maximum voltage is 13.84 V, and the average is 2.73 V.

Figures 14–16 show the measurement results for the simultaneous excitation at 2.3, 2.6 and 2.9 Hz periodic external forces and random vibrations. The voltages values increased significantly, with maximum voltages of 44.85, 46.35 and 44.29 V, and average values of 5.93, 9.08 and 9.49 V, respectively. The vibration displacement of the mass block increases significantly, and frequent bistable vibrations occur over the central axis, indicating stochastic resonance in this excitation frequency range. As a result, the predicted value of the excitation frequency in equation (23) agrees with experimental values.
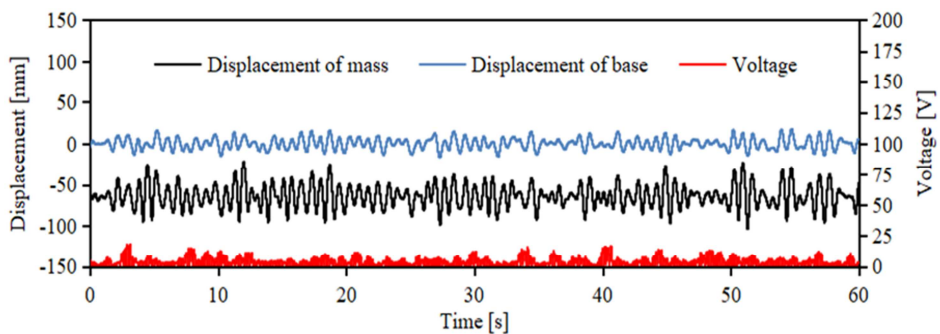

Figure 13. Experimental results of vibration displacements and voltage excited with random and 2.0 Hz periodic forces.
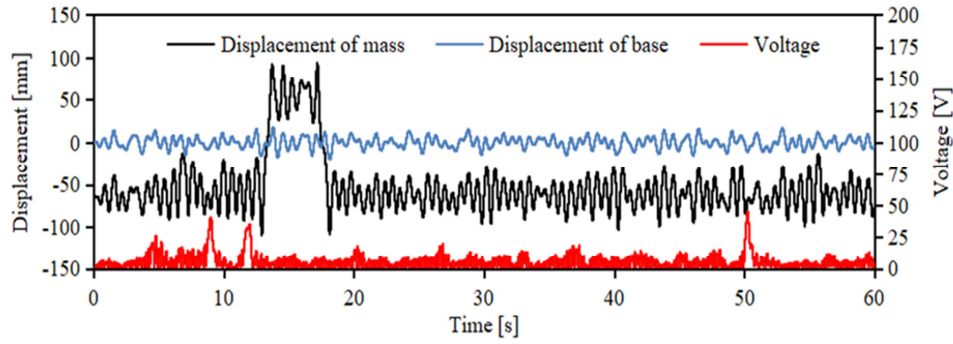
Figure 14. *Experimental results of vibration displacements and voltage excited with random and 2.3 Hz periodic forces.*
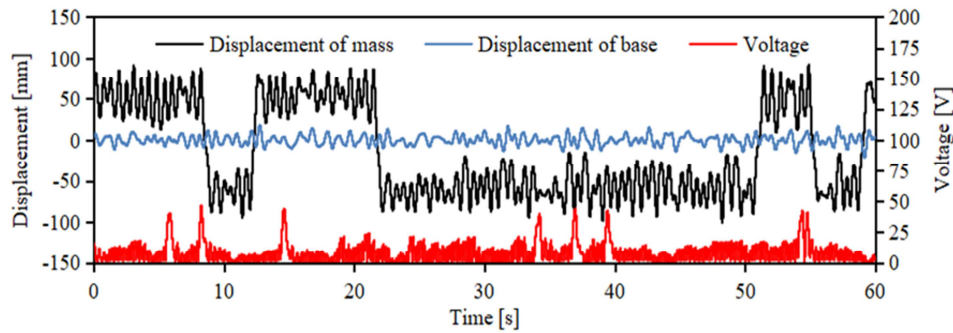

Figure 15. *Experimental results of vibration displacements and voltage excited with random and 2.6 Hz periodic forces.*

Figure 16. *Experimental results of vibration displacements and voltage excited with random and 2.9 Hz periodic forces.*

Figure 17. *Experimental results of vibration displacements and voltage excited with random and 3.2 Hz periodic forces.*

When the frequency of the periodic excitation signal is increased to 3.2 Hz, as shown in figure 17, the vibration of the mass block decreases, the bistable vibration disappears, and a single stable vibration state appears. The maximum voltage is 27.91 V, and the average is 7.14 V.

3.4. Amplification Effect by Stochastic Resonance

The amplification effect due to stochastic resonance is evaluated quantitatively, using the standard deviation of the vibration response displacement given by the following

equation:

$$S = \frac{1}{N} \sum_{i=1}^{N} (x_i - x_0)^2 \qquad (24)$$

where x_i is the vibration displacement; x_0 is the average value of the vibration displacement; and N is the number of sample points in the measurement experiment. Table 2 shows the standard deviation of the vibration displacement measurements.

The vibration displacement of the supporting point is used as a reference for comparison. The amplification of the stochastic resonance is evaluated using the increase rate of the standard deviation of the vibration displacement as an evaluation index.

As shown in Table 2, the average rate of increase of the displacement standard deviation when stochastic resonance does not occur is 186.64%. The average rate of increase of the displacement standard deviation when the stochastic resonance phenomenon occurs is 779.57%. The amplification effect due to stochastic resonance is very large.

Table 2. *Increasing rates of the motion response displacements under different vibrational states.*

Vibration signals		Mass	Base	Increasing	State
Only random		11.92	4.45	167.64%	
	2.0 Hz	10.49	5.04	108.13%	
	2.3 Hz	13.08	4.05	222.96%	
Periodic only	2.6 Hz	17.47	4.49	287.75%	Mono-stable
	2.9 Hz	13.63	3.66	272.40%	
	3.2 Hz	10.27	4.01	156.11%	
	2.0 Hz	14.47	6.64	117.92%	
	2.3 Hz	50.51	6.40	689.22%	
Random and periodic	2.6 Hz	57.15	5.95	860.50%	Bi-stable
	2.9 Hz	54.94	6.18	789.00%	
	3.2 Hz	16.22	6.23	160.35%	Mono-stable

3.5. Effect of Stochastic Resonance on Power Generation

The vibration power generation is evaluated using the average electrical power given by the following equation:

$$W = \frac{1}{T} \int \frac{V^2}{R} dt = \frac{\Delta t}{TR} \sum_{i=1}^{N} V_i^2 \qquad (25)$$

where V is the voltage, R is the electrical load resistance of the circuit, V_i is the measured voltage, Δt is the time step of the measurement, N is the number of samples of the measured value, and T is the total measurement time. Here, R is 1.0 MΩ, Δt is 0.001 s, and T is 60 s.

Table 3 shows the results of calculating the average electrical power W for each measured voltage value using equation (25). The vibration power generation is greatly increased due to the stochastic resonance.

For comparison, the sum of the electric power (0.031 mW) under random signal excitation and the electric power (0.091 mW) under periodic signal excitation at 2.6 Hz is 0.031+0.091=0.122 mW. However, the electric power obtained by the two-signal excitation is 0.148 mW.

Although the external excitation signal input is the same, the vibration electrical power generated by the two-signal excitation is approximately 21% larger than the sum of the vibration electrical power generated by separate excitations.

Table 3. *Comparison of the amount of vibration power generation under different vibrational states.*

Vibration signals		Electrical power [mW]	State
Only random		11.92	
	2.0 Hz	10.49	
	2.3 Hz	13.08	
Periodic only	2.6 Hz	17.47	Mono-stable
	2.9 Hz	13.63	
	3.2 Hz	10.27	
	2.0 Hz	14.47	
	2.3 Hz	50.51	
Random and periodic	2.6 Hz	57.15	Bi-stable
	2.9 Hz	54.94	
	3.2 Hz	16.22	Mono-stable

4. Conclusion

In this study, we proposed a new horizontal bi-stable vibration energy harvesting system, investigated its characteristics of stochastic resonance and vibration power generation, and obtained the following conclusions:

A new vibration-energy-harvesting experimental device was developed using a horizontal bistable vibration system and piezoelectric elements. Stochastic resonance was

generated in the bi-stable vibration system by combining random and periodic excitations. An average amplification effect of 779.57% was obtained for the relative vibration response of the support point.

The amount of electrical power generated when the random and periodic signals are simultaneously 21% higher than that generated when a single excitation is applied separately. It was found that stochastic resonance improved the efficiency of the vibration power generation.

From the nonlinear equation of motion of the bi-stable oscillatory system, the potential energy distribution exhibited a well characteristic. It is shown that the proposed vibration model has bi-stable vibration characteristics. A prediction equation for the periodic excitation frequency that induces stochastic resonance was derived. As confirmed by the measurement experiment, the periodic frequency under the stochastic resonance agrees with the predicted value.

The proposed bistable vibration system has a relatively simple structure. When used in a complex vibration environment, the motion of the mass block is guided by rails, which has the advantage of suppressing the perturbing effects of loads. This method can be used for developing future vibration-energy harvesting systems.

References

[1] Priya, S., Song, H., Zhou, Y., Varghese, R., Chopra, A., Kim, S., Kanno, I., Wu, L., Ha, D. S., Ryu J., & Polcawich R. D. (2017). A Review on Piezoelectric Energy Harvesting: Materials, Methods, and Circuits. Energy Harvesting and Systems, 4 (1), 791-796. doi:org/10.1515/ehs-2016-0028.

[2] Zhang, H., Corr, L. R., & Ma, T. (2018). Issues in vibration energy harvesting. Journal of Sound and Vibration, 421 (12), 79-90. doi:org/10.1016/j.jsv.2018.01.057.

[3] Jiang, J., Liu, S., Feng, L., & Zhao, D. (2021). A Review of Piezoelectric Vibration Energy Harvesting with Magnetic Coupling Based on Different Structural Characteristics. Micromachines, 12 (4), 436. doi:org/10.3390/mi12040436.

[4] Stephen, N. G. (2006). On energy harvesting from ambient vibration. Journal of Sound and Vibration, 293 (1), 409-425. doi:org/10.1016/j.jsv.2005.10.003.

[5] Khan, F., & Ahmad, I. (2016). Review of Energy Harvesters Utilizing Bridge Vibrations. Shock and Vibration, 2016, 1340402. doi:org/10.1155/2016/1340402.

[6] Lallart, M., Anton, S. R., & Inman, D. J. (2010). Frequency Self-tuning Scheme for Broadband Vibration Energy Harvesting. Journal of Intelligent Material Systems and Structures, 21 (9), 897-906. doi:org/10.1177/1045389X10369716.

[7] Kubba, A. E., & Jiang, K. (2014). Efficiency Enhancement of a Cantilever-Based Vibration Energy Harvester. Sensors, 14 (1), 188-211. doi:org/10.3390/s140100188.

[8] Dong, L., Grissom, M. & Fisher, F. T. (2015). Resonant frequency of mass-loaded membranes for vibration energy harvesting applications. AIMS Energy, 3 (3), 344-359. doi: 10.3934/energy.2015.3.344.

[9] Chen, Z., He, J. & Wang, G. (2019). Vibration Bandgaps of Piezoelectric Metamaterial Plate with Local Resonators for Vibration Energy Harvesting. Shock and Vibration, 2019, 1397123. doi:org/10.1155/2019/1397123.

[10] Dai, X. (2016). An vibration energy harvester with broadband and frequency-doubling characteristics based on rotary pendulums. Sensors and Actuators A: Physical, 241, 161-168. doi: org/10.1016/j.sna.2016.02.004.

[11] Yang, W. & Towfighian, S. (2017). A hybrid nonlinear vibration energy harvester. Mechanical Systems and Signal Processing, 90, 317-333. doi: org/10.1016/j.ymssp.2016.12.032.

[12] Gafforelli, G., Corigliano, R., Xu, R., & Kim, S. (2014). Stochastic averaging of energy harvesting systems. Applied Physics Letters, 105, 203901. doi:org/10.1063/1.4902116.

[13] Gammaitoni, L., Neri, I., & Vocca, H. (2009). Nonlinear oscillators for vibration energy harvesting. Applied Physics Letters, 94, 164102. doi:org/10.1063/1.3120279.

[14] Jiang, W., & Chen, L. (2016). Stochastic averaging of energy harvesting systems. International Journal of Non-Linear Mechanics, 85, 174-187. doi: org/10.1016/j.ijnonlinmec.2016.07.002.

[15] McInnes, C. R., Gorman, D. G., & Cartmell, M. P. (2008). Enhanced Vibrational Energy Harvesting using Nonlinear Stochastic Resonance. Journal of Sound and Vibration, 318 (4), 655-662. doi: org/10.1016/j.jsv.2008.07.017.

[16] Gammaitoni, L., Hanggi, P., Jung, P., & Marchesoni, F. (1999). Stochastic resonance. Reviews of Modern Physics, 70, 223-287. doi:org/10.1103/RevModPhys.70.223.

[17] McNamara, B., & Wiesenfeld, K. (1989). Theory of stochastic resonance. Physical Review A, 39 (9), 4854-4869. doi:org/10.1103/PhysRevA.39.4854.

[18] Tretyakov, M. V. (1998). Numerical technique for studying stochastic resonance. Physical Review E, 57 (4), 4789-4794. doi:10.1103/PhysRevE.57.4789.

[19] Harne, R. L. & Wang, K. W. (2013). A review of the recent research on vibration energy harvesting via bistable systems. Smart Materials and Structures, 22, 023001. doi: 10.1088/0964-1726/22/2/023001.

[20] Pellegrini, S. P., Tolou, N., Schenk, M., & Herder, J. L. (2012). Bistable vibration energy harvesters: A review. Journal of Intelligent Material Systems and Structures, 24 (11), 1303-1312. doi:10.1177/1045389X12444940.

[21] Zheng, R., Nakano, K., Hu, H., Su, D. & Matthew, P. C. (2014). An Application of Stochastic Resonance for Energy Harvesting in a Bistable Vibrating System. Journal of Sound and Vibration, 333 (12), 2568-2587. doi:org/10.1016/j.jsv.2014.01.020.

[22] Zhang, Y., Zheng, R., Kaizuka, T., Su, D. & Nakano, K. (2015). Broadband vibration energy harvesting by application of stochastic resonance from rotational environments. The European Physical Journal Special Topics, 224, 2687-2701. doi: 10.1140/epjst/e2015-02583-7.

[23] Zuo, L., & Tang, X. (2013). Large-scale vibration energy harvesting. Journal of Intelligent Material Systems and Structures, 21 (11), 1405-1430. doi:org/10.1177/1045389X13486707.

[24] Zhao, W., Wu, Q., Zhao, X., Nakano, K., & Zheng, R. (2020). Development of large-scale bistable motion system for energy harvesting by application of stochastic resonance. Journal of Sound and Vibration, 473, 115213. doi: org/10.1016/j.jsv.2020.115213.

[25] Beer, F. B., Johnston, E. R., Deworf, J. T., & Mazurek, D. F. (2012). Mechanics of materials. McGraw Hill, 233-236.